

# Correlation Between Fat Attenuation Index and Plaque Parameters in Coronary CT Angiography: An Observational Study in Stable Coronary Artery Disease

Clinical and Applied  
Thrombosis/Hemostasis  
Volume 31: 1-9  
© The Author(s) 2025  
Article reuse guidelines:  
sagepub.com/journals-permissions  
DOI: 10.1177/10760296241313459  
journals.sagepub.com/home/cat



Ting Guo, MD<sup>1</sup>, Xiu-Ping Wang, BD<sup>2</sup>, Rui Xia, BD<sup>2</sup>, Zihan Gu, BD<sup>3</sup>,  
and Xiao-Feng Dou, MD<sup>2</sup>

## Abstract

**Background:** The purpose of this prospective observational study was to predict plaque vulnerability, stenosis, and hemodynamic problems based on coronary CT angiography (CCTA) using the Fat Attenuation Index (FAI) as a marker.

**Methods:** Patients with stable coronary artery disease (CAD) who underwent CCTA between January 2021 and January 2023 were included in this study. Data on basic patient information, plaque parameters, and Fractional Flow Reserve (FFR) were collected and analyzed. Multiple linear analysis was performed to explore the association between FAI and FFR. Additionally, regression models were developed to predict dependent variables such as FFR, plaque vulnerability, and the degree of stenosis based on FAI values. We also explored specific thresholds of FAI to classify plaques into vulnerable and non-vulnerable categories.

**Results:** A total of 62 patients with 84 coronary arteries were included in the final analysis. Based on FAI levels, the study subjects were divided into FAI-negative group (FAI  $\leq -70.1$  HU, 52 cases) and FAI-positive group (FAI  $> -70.1$  HU, 32 cases). Patients in the FAI-positive group had significantly lower FFR values compared to those in the FAI-negative group, and the proportion of vulnerable plaques was significantly higher in the FAI-positive group. Furthermore, as the degree of stenosis observed on CCTA increased, FAI values showed a significant increase. Analysis of plaque types revealed that FAI in vulnerable plaques was significantly higher than in other plaque types. In the multiple linear analysis, lesion length, TPB and FFR was negatively correlated with FAI ( $\beta = -0.25, -0.13$  and  $-41.72$ ).

**Conclusion:** The results support the use of FAI as a valuable tool in clinical practice. Its predictive capabilities regarding hemodynamic dysfunction and plaque susceptibility make it an essential component of modern cardiovascular risk assessment strategies.

## Keywords

coronary artery disease, fat attenuation index, perivascular adipose tissue, vulnerable plaques, fractional flow reserve

Date received: 18 September 2024; revised: 16 December 2024; accepted: 30 December 2024.

## Background

Perivascular adipose tissue (PVAT) encompasses the adipose tissue surrounding the majority of the vascular system and has emerged as a dynamic constituent of the vascular wall, playing a pivotal role in regulating vascular homeostasis and influencing the pathogenesis of atherosclerosis. PVAT originates from a distinct precursor and exhibits a close association with the vascular system.<sup>1</sup> In addition to adipocytes, PVAT harbors diverse populations of immune cells. Under physiological conditions, PVAT not only provides structural support to blood vessels and serves as an energy depot but also exhibits active endocrine functions, releasing a myriad of

<sup>1</sup>Institute of Clinical Medicine, The Affiliated Taizhou People's Hospital of Nanjing Medical University, Taizhou School of Clinical Medicine, Nanjing Medical University, Taizhou, China

<sup>2</sup>Medical Imaging Department, The Affiliated Taizhou People's Hospital of Nanjing Medical University, Taizhou School of Clinical Medicine, Nanjing Medical University, Taizhou, China

<sup>3</sup>Massey Institute, Nanjing University of Finance & Economics, Nanjing, China

### Corresponding Author:

Xiao-Feng Dou, Medical Imaging Department, The Affiliated Taizhou People's Hospital of Nanjing Medical University, Taizhou School of Clinical Medicine, Nanjing Medical University, No.366, Taihu Road, Pharmaceutical High-tech Zone, Taizhou, China.

Email: douxiaofeng\_3@126.com



Creative Commons Non Commercial CC BY-NC: This article is distributed under the terms of the Creative Commons

Attribution-NonCommercial 4.0 License (<https://creativecommons.org/licenses/by-nc/4.0/>) which permits non-commercial use,

reproduction and distribution of the work without further permission provided the original work is attributed as specified on the SAGE and Open Access page (<https://us.sagepub.com/en-us/nam/open-access-at-sage>).

adipokines and cytokines. These factors modulate the vascular and systemic immune microenvironment, exerting potent anti-atherosclerotic effects.<sup>2</sup> Conversely, under pathological conditions, dysregulated PVAT loses its thermogenic capacity, secretes pro-inflammatory adipokines, induces endothelial dysfunction, facilitates infiltration of inflammatory cells, fosters atherosclerosis development, and impacts plaque occurrence and stability.<sup>3,4</sup> The interplay between PVAT and the vascular wall is bidirectional and closely associated with calcification and adverse clinical outcomes.<sup>5</sup> In its pro-inflammatory state, PVAT secretes a variety of pro-inflammatory cytokines and adipokines, such as interleukin-6 (IL-6) and tumor necrosis factor- $\alpha$  (TNF- $\alpha$ ). Promoting the activation and adhesion of monocytes to the endothelium, which accelerates atherogenesis.<sup>6</sup> Enhancing the recruitment and retention of inflammatory cells, including macrophages, which ingest lipids and become foam cells, contributing to plaque growth. Chronic inflammation within the vessel wall leads to the degradation of the extracellular matrix by matrix metalloproteinase (MMP), weakening the fibrous cap and increasing the risk of plaque rupture.<sup>7</sup>

One of the main signaling pathways implicated in PVAT-induced inflammation is the nuclear factor-kappa B (NF- $\kappa$ B) pathway. When activated by pro-inflammatory stimuli, such as TNF- $\alpha$  or oxidative stress, NF- $\kappa$ B translocates into the nucleus and promotes the transcription of numerous inflammatory genes, including cytokines (eg, IL-6, TNF- $\alpha$ ), chemokines, and adhesion molecules, which exacerbate vascular inflammation and atherosclerosis.<sup>8</sup>

Another important signaling pathway is the Janus kinase/signal transducer and activator of transcription (JAK/STAT) pathway, which can be activated by IL-6 and contributes to pro-inflammatory responses in both endothelial cells and surrounding adipose tissue.<sup>9</sup>

The Perivascular Fat Attenuation Index (FAI) is a parameter derived from coronary CT angiography (CCTA) that captures the balance between lipid and water content within PVAT. As a novel imaging biomarker, FAI quantifies the attenuation gradient of conventional CCTA to reflect inflammatory activity in coronary arteries.<sup>10</sup> In the presence of vascular inflammation, adipogenesis is inhibited in favor of lipolysis, leading to increased water content in adipose cells. This process shifts the overall attenuation of perivascular adipose tissue on CT (measured in Hounsfield units) due to edema and serves as a useful biomarker for in vivo assessment of coronary inflammation. The CRISP-CT study demonstrated that elevated FAI around the vessels enhances the prediction of cardiac risk and improves the reclassification capabilities of traditional CCTA. When used together, FAI and plaque characteristics offer a multi-dimensional view of coronary artery disease by capturing both the inflammatory environment (FAI) and structural vulnerability (plaque parameters).<sup>11</sup> This combination could serve as a robust approach for predicting adverse cardiac events, leading to more informed decisions about patient management. These markers have the potential to shift the clinical paradigm from focusing solely on anatomical stenosis to a more dynamic, inflammation-driven model of atherosclerosis, which could

lead to earlier interventions and improved patient outcomes. Higher values of perivascular FAI (critical value  $\geq -70.1$  Hounsfield Units) are associated with an increased risk of cardiac death and adverse prognosis, underscoring the close correlation between changes in perivascular FAI and plaque stability.<sup>12</sup> The composition of atherosclerotic plaques correlates with FAI in terms of pathogenesis. FAI attenuation enables the detection of dynamic changes in PVAT in response to vascular inflammatory alterations and identifies vulnerable atherosclerotic plaques during acute coronary syndrome. Atherosclerosis impedes local intracellular lipid accumulation in perivascular adipose tissue, resulting in an elevation of FAI.<sup>13,14</sup> Existing studies have demonstrated a close association between FAI and the burden of non-calcified plaques. As the proportion of non-calcified components within the plaque increases and plaque volume expands, inflammation in the coronary arteries intensifies, leading to augmented perivascular fat density due to cellular edema and macrophage aggregation.<sup>15</sup> Nevertheless, the current understanding of the relationship between perivascular FAI and plaque parameters remains limited. Therefore, this study aims to investigate the association between CCTA-based perivascular FAI, plaque parameters, and hemodynamic abnormalities.

## Methods

### Study Participants

This prospective observational study included patients diagnosed with stable coronary artery disease (CAD) who underwent CCTA at our hospital between January 2021 and January 2023. Detailed demographic information, imaging data, and follow-up information were collected. The inclusion criteria were as follows: (1) Age between 18 and 80 years, composite diagnostic criteria for stable CAD; (2) Clear CCTA images with optimal contrast filling and absence of significant artifacts; (3) Patients presenting with symptoms such as angina or angina equivalent; (4) Presence of at least one lesion with a diameter stenosis between 30% and 90% in major epicardial vessels (diameter  $\geq 2$  mm) according to CCTA findings; (5) One week prior to admission, all patients should cease taking PCSK9 inhibitors, statins, and other drugs to prevent any impact on the outcomes of the examination; (6) Availability of complete general clinical and CCTA data. The exclusion criteria were as follows: (1) Age less than 18 years; (2) History of myocardial infarction; (3) History of coronary artery bypass grafting or stent placement; (4) Poor quality of CCTA images; (5) Anatomical variations in the heart or coronary arteries; (6) Concomitant rheumatoid arthritis or other conditions that can impact perivascular FAI, a. like obesity or an increase in body fat, can change the makeup of fat, which can affect FAI measures; b. Diabetes-related metabolic alterations can impact perivascular fat and other adipose tissue properties; c. The amount and makeup of fat that builds up around blood vessels can be impacted by abnormal blood lipid levels; d. Vascular and perivascular remodeling brought on by persistent hypertension may have an impact on FAI;

e. Metabolic diseases such as inflammation and uneven distribution of fat are frequently caused by renal failure. (7) Drugs like steroids and statins can change how fat is distributed and metabolized, which can have an impact on FAI measurement; FAI levels can be impacted by hormonal diseases, including hypothyroidism and Cushing's syndrome, which can cause aberrant fat distribution.

### **CCTA Examination Method**

CCTA examinations were performed using a dual-source CT scanner (SOMATOM Force CT, Germany) following these steps: (1) Pre-scan preparation: Coronary artery dilation was performed to minimize respiratory motion artifacts. Sublingual nitroglycerin spray was administered to all participants, except for those who were hypotensive (Systolic blood pressure below 90mmHg or diastolic blood pressure below 60mmHg), and they were instructed to hold their breath during the examination; (2) Contrast agent injection: Iodixanol (Bayer, Germany) was injected into the antecubital vein using a 20G catheter at a flow rate of 3.5-5.5 mL/s; (3) Scanning: Prospective electrocardiogram-triggered sequence was used for CCTA scanning. The scan was initiated 5 s after reaching an attenuation threshold of 100 Hounsfield Units (HU) in the aortic arch, using bolus tracking for contrast agent injection. The scan was performed during the 30%-80% of the R-R interval, and images were reconstructed with a slice thickness of 0.75 mm and a reconstruction interval of 0.5 mm; (4) Image post-processing: Optimal diastolic and systolic phases were automatically reconstructed.

### **Hemodynamic Assessment of Lesion Vessels**

After the CCTA, the invasive coronary angiography (ICA) was adopted subsequently. ICA was a medical procedure used to visualize the coronary arteries, which supply blood to the heart. It is considered the gold standard for diagnosing CAD, blockages, and other abnormalities in the heart's blood vessels. During ICA, fractional flow reserve (FFR) examination was conducted to evaluate hemodynamic changes. The procedure was performed via the femoral or radial artery route, and coronary artery stenosis was assessed by two experienced interventional cardiologists. FFR, defined as the ratio of pressure in the distal coronary artery during maximal hyperemia to aortic pressure, was measured using a pressure wire. FFR measurements were obtained approximately 2 cm distal to the stenosis under continuous intravenous adenosine infusion at a rate of 160 µg/kg/min to induce hyperemia. An FFR value of  $\leq 0.80$  was considered indicative of lesion-specific hemodynamic abnormality.

### **Analysis of Perivascular FAI Surrounding Plaques**

The analysis of perivascular FAI surrounding plaques was performed using the Easy FAI Intelligent Evaluation system of perivascular Fat software (Version 1.2.0, Shukun, China). Perivascular FAI was defined as the average CT attenuation

of the perivascular adipose tissue within the radial distance equivalent to the diameter of the target vessel from the outer vascular wall. The measurement range encompassed tissues with a density ranging from  $-190$  to  $-3$  Hounsfield Units (HU). The software automatically segmented the proximal 40 mm of each major coronary artery (left anterior descending artery, left circumflex artery, and right coronary artery) to ensure consistency in FAI measurement. Two experienced radiologists independently conducted measurements for each case, and any discrepancies were resolved by a senior physician. The radiologists were blinded to the clinical, CCTA, and FFR data of the participants. It has been established through research that a cut off of  $-70.1$  HU is linked to worse outcomes.<sup>16</sup> As a result, the threshold for this investigation was  $-70.1$  HU, and the participants were divided into two groups: the FAI-positive group ( $\text{FAI} > -70.1$  HU) and the FAI-negative group ( $\text{FAI} \leq -70.1$  HU).

### **Analysis of Plaque Composition**

CCTA images of good quality were selected for further post-processing and plaque analysis. Plaque characteristics included the following: (1) Remodeling index (RI), defined as the ratio of the cross-sectional area of the vascular lesion to the proximal reference vessel area, where positive remodeling (PR) was defined as  $\text{RI} > 1.0$ ; (2) Maximum diameter stenosis (MDS), calculated as the minimum luminal diameter divided by the reference diameter and multiplied by 100%; (3) Total plaque burden (TPB), determined as the plaque volume divided by the vessel volume and multiplied by 100%; (4) Calcified plaques (CP, with a threshold of 376-1300 HU); (5) Non-calcified plaques (NCP, with a threshold of  $-30$ -375 HU). Plaques demonstrating both calcified and non-calcified features were classified as mixed plaques.

### **Vulnerable Plaque Characteristics**

Based on the CT imaging results, vulnerable plaques were defined as plaques exhibiting at least two or more of the following high-risk features:<sup>16</sup> positive remodeling, spotty calcification (calcification within a plaque with a diameter less than 3 mm), low-attenuation NCP (L-NCP), and the napkin ring sign (a high-density ring-shaped area surrounding a low-density plaque).

### **Statistical Analysis**

Statistical analysis was conducted using SPSS 22.0 and R software. The assumption of normal distribution was assessed using the Shapiro-Wilk test for quantitative data. Quantitative variables with a normal distribution were presented as mean  $\pm$  standard deviation ( $\bar{x} \pm s$ ), while non-normally distributed variables were presented as median and interquartile range. The t-test and Mann-Whitney U test were employed for statistical analysis of normally distributed and non-normally distributed variables, respectively. The data subjected to t-test were subjected to Levene's test for similarity and normal distribution.

Categorical data were expressed as rates, and the chi-square test was performed for statistical analysis. Multiple linear regression analysis was performed to determine the independent factors significantly associated with FAI, while adjusting for potential confounders. Based on the results of the univariate analysis, variables with a *P*-value of less than .1 were selected for inclusion in the multiple analysis model. This liberal criterion allowed for the consideration of variables that may not have reached the conventional significance level (eg, *P* < .05) but still exhibited some evidence of association with the outcome variable. This method provided insights into the complex

relationships among variables, ensuring that potentially important factors were not prematurely excluded based on a more stringent *P*-value threshold in the univariate analysis.

## Results

### Clinical Characteristics

Sample size calculation was conducted based on a case-control study design using a hospital-based sampling survey. The estimated prevalence of the disease is 5%, with a relative sampling error of 20%. The design effect (deff) was set at 1.5, referencing the National Guidelines for the Management of Cardiovascular Diseases and other similar large-scale health surveys. A 95% confidence interval was applied, with *Z*<sub>α</sub> = 1.96. Additionally, a 15% rate of incomplete data was considered. The final calculated sample size falls within the range of 50 to 100.

A total of 62 patients with a total of 84 coronary arteries were included in the analysis. The patients had an average age of 63.25 ± 10.61 years, with 20 males and 42 females. The average body mass index (BMI) was 25.36 ± 3.69 kg/m<sup>2</sup>. Among the patients, 35 had hypertension, 20 had diabetes, 26 had hyperlipidemia, and 18 had a history of smoking. Lesions were found in 60 left anterior descending arteries (LAD), 10 left circumflex arteries (LCX), and 14 right coronary arteries (RCA). Table 1 shows the clinical characteristics of the included patients.

### Comparison of Plaque Characteristics at Different FAI Levels

The study subjects were divided into two groups based on FAI levels: the FAI-negative group (FAI ≤ -70.1 HU, 52 cases) and

**Table 1.** Clinical Characteristics of Included Patients.

Characteristics	Value	Percentage (%)
Number of participants	62	
Number of affected vessels	84	
Age[years( $\bar{x} \pm s$ )]	63.25 ± 10.61	
Sex [%( <i>n</i> )]		
Male	20	32.26
Female	42	67.74
Body mass index[kg/m <sup>2</sup> ( $\bar{x} \pm s$ )]	25.36 ± 3.69	
Cardiovascular risk factors[%( <i>n</i> )]		
Hypertension	35	56.45
Diabetes	20	32.26
Hyperlipidemia	26	41.94
History of smoking	18	29.03
Lesion location[%( <i>n</i> )]		
LAD	60	71.43
LCX	10	11.90
RCA	14	16.67

Abbreviations: LAD, anterior descending artery; LCX, left circumflex artery; RCA, right coronary artery.

**Table 2.** Comparison of Plaque Characteristics at Different FAI Levels.

Characteristics	FAI ≤ -70.1 HU (negative group)	FAI > -70.1 HU (positive group)	$\chi^2/t$	<i>P</i>
Number of vessels	52	32		
Lesion location[%( <i>n</i> )]			0.646	.724
LAD	69.23(36)	75.00(24)		
LCX	11.54(6)	12.50(4)		
RCA	19.23(10)	12.50(4)		
Lesion length[mm( $\bar{x} \pm s$ )]	22.36 ± 6.31	24.69 ± 6.28	1.646	.104
MDS[%( $\bar{x} \pm s$ )]	54.96 ± 17.25	59.36 ± 18.96	1.093	.278
TPB[%( $\bar{x} \pm s$ )]	54.23 ± 12.32	58.96 ± 11.82	1.735	.086
Plaque types[%( <i>n</i> )]			5.207	.074
Calcified plaques	33.85(22)	20.83(10)		
non-calcified plaques	18.46(12)	31.25(15)		
Mixed plaques	27.70(18)	14.58(7)		
Vulnerable plaques	20.00(13)	33.33(16)		
Characteristics of high-risk plaque[%( <i>n</i> )]			5.477	.019
Positive remodeling plaque	36.73(18)	42.31(11)		
Spot-like Calcification	30.61(15)	23.08(6)		
L-NCP	22.45(11)	19.23(5)		
Napkin-ring sign	10.20(5)	15.38(4)		
FFR( $\bar{x} \pm s$ )	0.846 ± 0.069	0.784 ± 0.073	3.902	.026

Abbreviations: FAI, fat Attenuation Index; LAD, anterior descending artery; LCX, left circumflex artery; RCA, right coronary artery; MDS, mean density score; TPB, total plaque burden; L-NCP, low-attenuation non-calcified plaque; FFR, fractional flow reserve.

the FAI-positive group ( $FAI > -70.1$  HU, 32 cases). Table 2 presents the plaque composition characteristics of the two groups. In the FAI-negative group, 36 lesions were found in the LAD, 6 in the LCX, and 10 in the RCA. The average lesion length was  $22.36 \pm 6.31$  mm. The percentage of plaque volume occupied by low-attenuation plaque to as mean density score(MDS) was  $54.96 \pm 17.25\%$ , and the percentage of total plaque burden (TPB) was  $54.23 \pm 12.32\%$ . The plaque types included 22 calcified plaques, 12 non-calcified plaques, and 18 mixed plaques. There were 16 vulnerable plaques, and the average fractional flow reserve (FFR) was  $0.846 \pm 0.069$ , with 7 plaques having  $FFR < 0.75$ . In the FAI-positive group, there were 24 lesions in the LAD, 4 in the LCX, and 4 in the RCA. The average lesion length was  $24.69 \pm 6.28$  mm. The MDS was  $59.36 \pm 18.96\%$ , TPB was  $58.96 \pm 11.82\%$ . Among the plaque types, there were 10 calcified plaques, 15 non-calcified plaques, and 7 mixed plaques. There were 13 vulnerable plaques, and the average FFR was  $0.784 \pm 0.073$ , with 7 plaques having  $FFR < 0.75$ . The FAI-positive group had significantly lower FFR and a higher proportion of vulnerable plaques compared to the FAI-negative group (all  $P < .05$ ), while other plaque composition characteristics showed no significant differences (all  $P > .05$ ).

### Comparison of FAI at Different Stenosis Levels

There were 15 subjects in mild stenosis (MDS 30%~50%) with the FAI of  $-82.16 \pm 9.77$ ; 21 subjects in moderate stenosis (MDS 51%~70%) with the FAI of  $-76.36 \pm 7.69$  and 48 subjects in severe stenosis (MDS 71%~90%) with the FAI of  $-71.68 \pm 8.36$ . There was significant difference between mild

stenosis and moderate stenosis ( $MD = -6.91$ , 95%CI:  $-8.01$ ,  $-5.81$ ) as well as the moderate stenosis and severe stenosis ( $MD = -4.82$ , 95%CI:  $-8.76$ ,  $-0.88$ ). The results are shown in Figure 1.

### Comparison of FFR and FAI in Different Plaque Types

The differences in FFR and FAI among different plaque types were analyzed, and the results are shown in Table 3. In vulnerable plaques, the average FAI was  $-71.48 \pm 6.39$ , and the average FFR was  $0.804 \pm 0.085$ . In other plaques, the average FAI was  $-75.56 \pm 7.76$ , and the average FFR was  $0.832 \pm 0.070$ . The FAI in vulnerable plaques was significantly higher than in other plaques ( $MD = -4.086$ , 95%CI:  $-7.42$ ,  $-0.74$ ), while there was no significant difference in FFR between the two types of plaques ( $MD = 0.028$ , 95%CI:  $-0.006$ ,  $0.062$ ).

### Linear Regression Analysis of Influencing Factors of FAI

In the multiple linear analysis examining factors associated with FAI, lesion length was inversely related to the outcome, with each unit increase in lesion length corresponding to a reduction in FAI ( $\beta = -0.25$ ; 95% CI,  $-0.45$  to  $-0.05$ ;  $P = .019$ ). Similarly, TPB was associated with a decrease in FAI, where each unit increase in TPB resulted in a decrease in FAI ( $\beta = -0.13$ ; 95% CI,  $-0.23$  to  $-0.03$ ;  $P = .010$ ). Notably, a negative correlation was observed between FAI and FFR, reinforcing that higher FAI values were associated with more significant hemodynamic abnormalities. For each unit increase in FFR, there was a marked decrease in the outcome ( $\beta = -41.72$ ; 95% CI,  $-57.26$  to  $-26.18$ ;  $P < 0.001$ ). This finding underscored that higher FAI levels in vulnerable plaques supported its utility as a marker of plaque instability. The results were shown in Table 4 and Figure 2.

### Discussion

Atherosclerosis is a complex inflammatory process that plays a critical role in the development and progression of plaque formation.<sup>17</sup> Adipose tissue surrounding the coronary arteries, known as PVAT, has been found to interact with the vessel wall through the secretion of paracrine factors.<sup>18</sup> Under normal conditions, PVAT secretes substances that promote vasodilation, possess anti-inflammatory and antioxidant properties, and contribute to vascular protection. However, in the

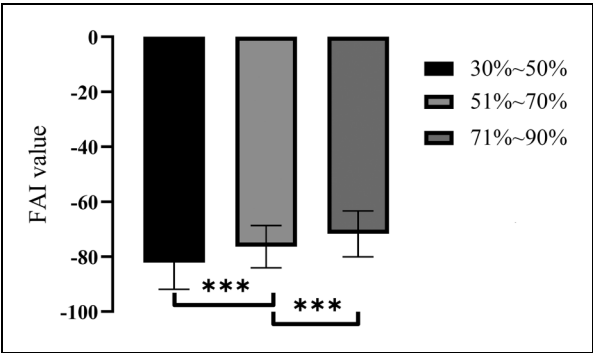


**Figure 1.** Comparison of FAI at different degrees of stenosis.

**Table 3.** Comparison of FFR and FAI in Different Plaque Types.

	Number of plaques	FAI	FFR
Vulnerable plaques	29	$-71.48 \pm 6.39$	$0.804 \pm 0.085$
Other plaques	55	$-75.56 \pm 7.76$	$0.832 \pm 0.070$
Mean deviation (95%CI)		$-4.086 (-7.42, -0.74)$	$0.028 (-0.006, 0.062)$
T		2.428	1.622
P		.017	.109

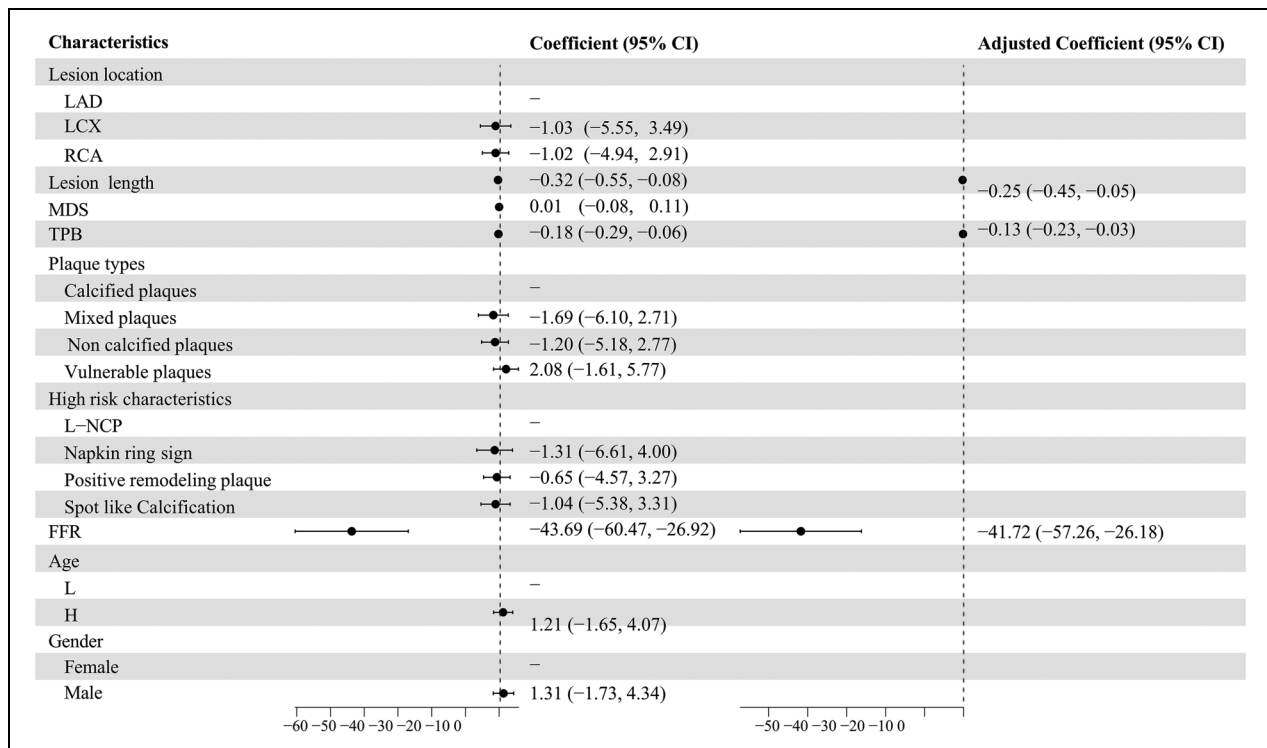
Abbreviations: FAI, fat Attenuation Index; FFR, fractional flow reserve.

**Table 4.** Univariate and Multiple Linear Analysis of Influencing Factors.

Characteristic	Univariable			Multivariable		
	Beta	95% CI	P-value	Beta	95% CI	P-value
Lesion location						
LAD	—	—				
LCX	−1.03	−5.55, 3.49	.656			
RCA	−1.02	−4.94, 2.91	.613			
Lesion length	−0.32	−0.55, −0.08	.010*	−0.25	−0.45, −0.05	.019*
MDS	0.01	−0.08, 0.11	.773			
TPB	−0.18	−0.29, −0.06	.003**	−0.13	−0.23, −0.03	.010*
Plaque types						
Calcified plaques	—	—				
Mixed plaques	−1.69	−6.10, 2.71	.453			
Non-calcified plaques	−1.20	−5.18, 2.77	.555			
Vulnerable plaques	2.08	−1.63, 5.79	.275			
High risk characteristics						
L-NCP	—	—				
Napkin-ring sign	−1.31	−6.61, 4.00	.631			
Positive remodeling plaque	−0.65	−4.57, 3.27	.746			
Spot-like Calcification	−1.04	−5.38, 3.31	.641			
FFR	−43.69	−60.47, −26.92	<.001***	−41.72	−57.26, −26.18	<.001***
Age						
Low [31, 54]	—	—				
High [55,79]	0.91	−1.95, 3.78	.534			
Gender						
Female	—	—				
Male	1.31	−1.73, 4.34	.401			

Abbreviations: CI, Confidence Interval; LAD, anterior descending artery; LCX, left circumflex artery; RCA, right coronary artery; MDS, mean density score; TPB, total plaque burden; L-NCP, low-attenuation non-calcified plaque; FFR, fractional flow reserve.

\* $P < .05$ ; \*\* $P < .01$ ; \*\*\* $P < .001$ .

**Figure 2.** Forest plots of univariate and multivariate analysis.

presence of atherosclerotic plaques, this balance is disrupted, and PVAT undergoes phenotypic changes from a protective to an inflammatory state, leading to alterations in the local micro-environment.<sup>19</sup> Likewise, changes in PVAT can also impact the vessel wall, accelerating plaque progression and increasing plaque instability.<sup>20</sup> Anatomical studies have shown that PVAT surrounding plaques in patients who experienced adverse cardiovascular events contains a high number of inflammatory cells, and pathological studies have confirmed the involvement of periplaque adipose tissue inflammation in plaque formation and progression.<sup>21</sup> The FAI, measured using CCTA, assesses and quantifies the compositional changes in PVAT by evaluating spatial variations in fat density. It serves as a sensitive and dynamic biomarker for perivascular inflammation.<sup>22</sup>

The findings of this study revealed no significant differences in plaque length, volume, and plaque type between the FAI-positive and FAI-negative groups. However, the proportion of vulnerable plaques was significantly higher in the FAI-positive group. In vulnerable plaques, the FAI value around the plaque was significantly higher than in other plaques. Moreover, as stenosis severity increased, the FAI value around the plaque also significantly increased. As Bentzon et al<sup>23</sup> had shown in these results suggest that plaque size is not directly associated with plaque rupture, but rather plaque inflammation and morphology are closely linked to vulnerable plaques, ischemic events, and mortality rates. Plaques of varying lengths and volumes may undergo inflammatory reactions, and plaque inflammation itself is a manifestation of plaque progression.<sup>23</sup> Another study by Jing et al investigated PVAT differences among patients with different plaque types using quantitative parameters and found no intergroup differences in FAI related to age, gender, body mass index, risk factors, and plaque location. However, they observed the lowest FAI in non-calcified plaques.<sup>24</sup> Similarly, Goeller et al conducted a case-control study and found that culprit lesion vessels exhibited the highest FAI attenuation. Combining quantitative adverse plaque features with FAI attenuation can more reliably identify vulnerable plaques, which aligns with the findings of the current study.<sup>25</sup> Kuneman et al demonstrated that FAI attenuation around culprit vessels significantly increased compared to non-culprit vessels and stable coronary artery disease lesions, indicating higher inflammation intensity.<sup>26</sup>

Prior to CAD testing, CCTA is the recommended imaging modality for symptomatic patients with low likelihood. The most recent generation of CT scanners can identify CAD with excellent diagnostic accuracy even in individuals with irregular cardiac patterns or a fast heart rate because they can achieve good image quality while lowering contrast and radiation dosage. The FAI of adipose tissue surrounding plaques, based on CCTA, can assess plaque features and stratify the risk of CAD patients according to the severity of coronary artery stenosis.<sup>27</sup> According to Bergamaschi et al,<sup>27</sup> baseline plaque burden predicts the development of obstructive CAD and is linked to the risk of significant cardiovascular events regardless of the existence of obstructive lesions. Physicians will concentrate on secondary healthcare since the features of high-risk plaques—such as positive remodeling,

low attenuation plaques, napkin ring sign, and spot calcification—are strong predictors of subsequent myocardial infarction.<sup>28</sup>

The present study confirms and expands upon previous research, particularly by analyzing the correlation between FAI and FFR. The results revealed a significant negative correlation between FAI and FFR in all plaques, and this correlation was even stronger in vulnerable plaques. Another study by Ma et al found that overall FAI was not significantly correlated with abnormal FFR, but lesion-specific PVAT was independently correlated with abnormal FFR.<sup>28</sup> The current study focused on the area surrounding the plaque, which is consistent with the findings of Ma et al. Although this study did not explore the relationship between FAI and prognosis, research has demonstrated that FAI is associated with an increased risk of all-cause mortality, cardiac mortality, and adverse clinical outcomes. Additionally, FAI can aid in detecting culprit lesions in patients with acute myocardial infarction.<sup>12,29</sup> Studies have also shown that a decrease in CT-FFR and an increase in FAI during follow-up CCTA are strong predictors of cardiovascular events, providing higher prognostic value for risk stratification compared to conventional clinical and imaging parameters.<sup>30</sup>

The Coronary Artery Calcium (CAC) Score is widely used to quantify calcified atherosclerotic plaques in the coronary arteries. It has proven to be a strong predictor of future cardiovascular events, particularly in asymptomatic patients. Higher CAC scores indicate a higher burden of calcified plaque and, by extension, a higher risk of coronary events. While the CAC score is valuable in detecting calcified plaques, it does not provide information about non-calcified, vulnerable plaques, which are more prone to rupture and cause acute events. Moreover, it does not capture the inflammatory activity within the coronary arteries, which plays a crucial role in the progression of atherosclerosis and plaque instability.<sup>31</sup> FAI complements the CAC score by providing additional information about the inflammatory environment of the coronary arteries. FAI detects perivascular inflammation, which is associated with the presence of vulnerable, non-calcified plaques—those that may not contribute significantly to the CAC score but pose a high risk of rupture. By integrating FAI with CAC scoring, clinicians can obtain a more comprehensive risk profile, identifying both the burden of calcified plaques and the presence of underlying inflammation, which could guide more personalized treatment strategies.

In asymptomatic patients, the CAC score remains a valuable tool for early detection of coronary artery disease, identifying those at risk even before clinical symptoms emerge. Adding FAI to this assessment enhances the ability to detect patients with active, inflammation-driven disease, who might be missed by CAC alone. This synergy can aid in identifying high-risk individuals earlier and prevent the development of acute coronary events.<sup>32</sup>

In patients with known CAD, combining FAI with plaque volume and composition data provides a more complete picture of disease progression. Plaque volume quantifies the overall burden, while FAI highlights inflammation, indicating areas of the vessel wall that may harbor vulnerable plaques. This combination can help clinicians better identify which

patients are at higher risk for plaque rupture and guide decisions regarding more aggressive interventions or closer follow-up.

## Conclusion

The results indicate a relationship between FAI, vulnerable plaques, stenosis severity, and hemodynamic abnormalities. However, given that this is a single-centered study with a relatively small sample size, these conclusions should be interpreted with caution. Further multi-centered studies with larger populations are needed to confirm these associations and establish the broader applicability of FAI as a reliable diagnostic tool.

## Acknowledgements

We would like to acknowledge the hard and dedicated work of all the staff that implemented the intervention and evaluation components of the study.

## Authors' Contributions

Ting Guo and Xiao-Feng Dou conceived the idea and conceptualised the study. Xiu-Ping Wang collected the data. Rui Xia and Zihan Gu analysed the data. Ting Guo and Xiao-Feng Dou drafted the manuscript, then Ting Guo and Xiao-Feng Dou reviewed the manuscript. All authors read and approved the final draft.

## Availability of Data and Materials

The data that support the findings of this study are available from the corresponding author, upon reasonable request.

## Declaration of Conflicting Interests

The authors declared no potential conflicts of interest with respect to the research, authorship, and/or publication of this article.


## Ethics Approval and Consent to Participate

This study was conducted with approval from the Ethics Committee of The Affiliated Taizhou People's Hospital of Nanjing Medical University. This study was conducted in accordance with the declaration of Helsinki. Written informed consent was obtained from all participants.

## Funding

The authors received no financial support for the research, authorship, and/or publication of this article.

## ORCID iD

Xiao-Feng Dou  <https://orcid.org/0009-0003-6476-4392>

## References

- Nosalski R, Guzik TJ. Perivascular adipose tissue inflammation in vascular disease. *Br J Pharmacol*. 2017;174(20):3496-3513.
- Antoniades C, Tousoulis D, Vavlukis M, et al. Perivascular adipose tissue as a source of therapeutic targets and clinical biomarkers. *Eur Heart J*. 2023;44(38):3827-3844.
- Cheng CK, Ding H, Jiang M, Yin H, Gollasch M, Huang Y. Perivascular adipose tissue: Fine-tuner of vascular redox status and inflammation. *Redox Biol*. 2023;62(1):102683.
- Kim HW, Shi H, Winkler MA, Lee R, Weintraub NL. Perivascular adipose tissue and vascular perturbation/atherosclerosis. *Arterioscler Thromb Vasc Biol*. 2020;40(11):2569-2576.
- Margaritis M, Sanna F, Lazaros G, et al. Predictive value of telomere length on outcome following acute myocardial infarction: Evidence for contrasting effects of vascular vs. blood oxidative stress. *Eur Heart J*. 2017;38(41):3094-3104.
- Gruzdeva OV, Dyleva YA, Belik EV, et al. Relationship between epicardial and coronary adipose tissue and the expression of adiponectin, leptin, and interleukin 6 in patients with coronary artery disease. *J Pers Med*. 2022;12(2):129.
- Raffetto JD, Khalil RA. Mechanisms of lower extremity vein dysfunction in chronic venous disease and implications in management of varicose veins. *Vessel Plus*. 2021;5(1):36.
- Efferth T, Oesch F. The immunosuppressive activity of artemisinin-type drugs towards inflammatory and autoimmune diseases. *Med Res Rev*. 2021;41(6):3023-3061.
- Zhu H, Zhang H, Lu K, et al. Chlorinated organophosphate flame retardants impair the lung function via the IL-6/JAK/STAT signaling pathway. *Environ Sci Technol*. 2022;56(24):17858-17869.
- Chan K, Wahome E, Tsiachristas A, et al.; ORFAN Consortium. Inflammatory risk and cardiovascular events in patients without obstructive coronary artery disease: The ORFAN multicentre, longitudinal cohort study. *Lancet*. 2024;403(10444):2606-2618.
- Zhang R, Ju Z, Li Y, Gao Y, Gu H, Wang X. Pericoronary fat attenuation index is associated with plaque parameters and stenosis severity in patients with acute coronary syndrome: A cross-sectional study. *J Thorac Dis*. 2022;14(12):4865-4876.
- Oikonomou EK, Marwan M, Desai MY, et al. Non-invasive detection of coronary inflammation using computed tomography and prediction of residual cardiovascular risk (the CRISP CT study): A post-hoc analysis of prospective outcome data. *Lancet*. 2018;392(10151):929-939.
- Antonopoulos AS, Sanna F, Sabharwal N, et al. Detecting human coronary inflammation by imaging perivascular fat. *Sci Transl Med*. 2017;9(398):2568.
- Zuo L, Tian Z, Zhou B, et al. Perivascular fat attenuation index value and plaque volume increased in non-target lesions of coronary arteries after stenting. *Eur Radiol*. 2024;34(7):4233-4242.
- Goeller M, Tamarappoo BK, Kwan AC, et al. Relationship between changes in pericoronary adipose tissue attenuation and coronary plaque burden quantified from coronary computed tomography angiography. *Eur Heart J Cardiovasc Imaging*. 2019;20(6):636-643.
- Oikonomou EK, Marwan M, Desai MY, et al. Non-invasive detection of coronary inflammation using computed tomography and prediction of residual cardiovascular risk (the CRISP CT study): A post-hoc analysis of prospective outcome data. *Lancet*. 2018;392(10151):929-939.
- Yan H, Zhao N, Geng W, Hou Z, Gao Y, Lu B. The Perivascular Fat Attenuation Index Improves the Diagnostic Performance for Functional Coronary Stenosis. *J Cardiovasc Dev Dis*. 2022;9(5):128.



18. Margaritis M, Antonopoulos AS, Digby J, et al. Interactions between vascular wall and perivascular adipose tissue reveal novel roles for adiponectin in the regulation of endothelial nitric oxide synthase function in human vessels. *Circulation*. 2013;127(22):2209-2221.
19. Elnabawi YA, Oikonomou EK, Dey AK, et al. Association of biologic therapy with coronary inflammation in patients with psoriasis as assessed by perivascular fat attenuation Index. *JAMA Cardiol*. 2019;4(9):885-891.
20. Kuno T, Arce J, Fattouh M, et al. Cardiometabolic predictors of high-risk CCTA phenotype in a diverse patient population. *Am J Prev Cardiol*. 2023;15(1):100578.
21. Conte M, Petraglia L, Poggio P, et al. Inflammation and cardiovascular diseases in the elderly: The role of epicardial adipose tissue. *Front Med (Lausanne)*. 2022;9(1):844266.
22. Klüner LV, Oikonomou EK, Antoniadou C. Assessing cardiovascular risk by using the fat attenuation Index in coronary CT angiography. *Radiol Cardiothorac Imaging*. 2021;3(1):e200563.
23. Bentzon JF, Otsuka F, Virmani R, Falk E. Mechanisms of plaque formation and rupture. *Circ Res*. 2014;114(12):1852-1866.
24. Jing M, Sun J, Zhou Q, et al. Pericoronary adipose tissue differences among plaque types: A retrospective assessment. *Clin Imaging*. 2023;96(1):58-63.
25. Goeller M, Achenbach S, Cadet S, et al. Pericoronary adipose tissue computed tomography attenuation and high-risk plaque characteristics in acute coronary syndrome compared with stable coronary artery disease. *JAMA Cardiol*. 2018;3(9):858-863.
26. Kuneman JH, van Rosendaal SE, van der Bijl P, et al. Pericoronary adipose tissue attenuation in patients with acute coronary syndrome versus stable coronary artery disease. *Circ Cardiovasc Imaging*. 2023;16(2):e014672.
27. Bergamaschi L, Pavon AG, Angeli F, et al. The role of non-invasive multimodality imaging in chronic coronary syndrome: Anatomical and functional pathways. *Diagnostics (Basel)*. 2023;13(12):2083.
28. Feng Y, Xu Z, Zhang L, et al. Machine-learning-derived radiomics signature of pericoronary tissue in coronary CT angiography associates with functional ischemia. *Front Physiol*. 2022;13(1):980996.
29. Sayama K, Sugiyama T, Kanaji Y, et al. Prognostic utility of the pericoronary fat attenuation index in patients with takotsubo cardiomyopathy. *J Cardiovasc Comput Tomogr*. 2023;17(6):413-420.
30. Dai X, Hou Y, Tang C, et al. Long-term prognostic value of the serial changes of CT-derived fractional flow reserve and perivascular fat attenuation index. *Quant Imaging Med Surg*. 2022;12(1):752-765.
31. Xie Y, Shen H, Xu Q, et al. Evaluating coronary arteries and predicting MACEs using CCTA in lung cancer patients receiving chemotherapy or chemoradiotherapy. *Radiother Oncol*. 2024;200(1):110498.
32. Kim C, Aroda VR, Goldberg RB, et al. Diabetes Prevention Program Outcomes Study Group. Androgens, irregular menses, and risk of diabetes and coronary artery calcification in the diabetes prevention program. *J Clin Endocrinol Metab*. 2018;103(5):486-496.